

# The effect of normal electric fields on the Stokes drift

Marcelo V. Flamarion<sup>1</sup>, Luiz P. Palacio<sup>2</sup>, Roberto Ribeiro-Jr<sup>2</sup>

<sup>1</sup>Departamento Ciencias-Sección Matemáticas, Pontificia Universidad Católica del Perú, Av. Universitaria 1801, San Miguel 15088, Lima, Peru

mvellosoflamarionvasconcellos@pucp.edu.pe

<sup>2</sup>UFPR/Federal University of Paraná, Departamento de Matemática, Centro Politécnico, Jardim das Américas, Caixa Postal 19081, Curitiba, PR, 81531-980, Brazil

luizpalacio@ufpr.br

## Abstract

In periodic wave motion, particles beneath the wave undergo a drift in the direction of wave propagation, a phenomenon known as Stokes drift. While extensive research has been conducted on Stokes drift in water wave flows, its counterpart in electrohydrodynamic flows remains relatively unexplored. Addressing this gap, we investigate Stokes drift beneath periodic traveling irrotational waves on a dielectric fluid under the effect of normal electric fields. Through numerical simulations utilizing conformal mapping, we compute particle trajectories and analyze the resultant Stokes drift behaviors beneath periodic traveling waves. Our findings indicate that variations in the electric field impact particle velocities while maintaining trajectory shapes. Moreover, the kinetic energy associated with a particle depends on its depth location and is a non-decreasing convex function in a moving frame and a constant in a laboratory frame.

## 1 Introduction

The study of particle trajectories beneath a surface water wave dates back to 1839, and it is a problem of great physical and mathematical interest, being relevant for various applications, such as submarine operations, dispersion of pollutants, among others [25].

Historically, George Green [19] was the pioneer in the study of particle trajectories beneath a free surface wave. He proved that the particle trajectories beneath a linear wave in the deep water regime are circular and closed, with the radius decreasing exponentially with depth. Shortly after, George Biddell Airy [3] deduced that in finite depth, these paths are elliptical. Green's work inspired one of the most important figures in fluid dynamics, George Gabriel Stokes, who was mentored by William Hopkins at Cambridge. In autobiographical notes, Stokes recalled [10]:

I thought I would try my hand at original research; and, following a suggestion made to me by Mr. Hopkins while reading for my degree, I took up the subject of Hydrodynamics, then at rather a low ebb in the general reading of the place, notwithstanding that George Green, who had done admirable work in this and other departments, was resident in the University till he died. (Larmor 1907, p.8)

Stokes [26] deepened Green's studies using successive approximations, showing that in both shallow and deep water regimes, the particles beneath a wave undergo a drift in the direction of wave propagation, which was later called *Stokes Drift*. In this way, he conjectured that particle paths are not closed.

Years later, additional findings related to Stokes' conjecture were made. Ursell [28] proved that the paths of particles are not closed for waves in either shallow or deep water regimes with uniform depth. Longuet-Higgins [24] conducted an experimental study to determine the trajectory of a particle on the surface and found loop-shaped orbits with a drift in the direction of wave propagation. Constantin [7] provided a rigorous proof for Stokes' conjecture; in other words, he proved that particles beneath a wave undergo a drift in the direction of wave propagation in both shallow and deep water regimes and showed the geometry of the particle paths, which are loop-shaped. Constantin and Villari [8] analyzed a more specific case involving linear waves, where the velocity field of the fluid is known, and obtained the same result as in [7]. Constantin and Strauss [9] studied particle trajectories originating from the interaction of the free surface wave with a uniform current, and in this case, they proved that it is possible for the particles not to undergo a drift.

In more recent studies, significant progress has been made on various problems involving particle trajectories beneath free surface waves in reduced models [1, 4, 14, 15, 22]. Some authors have focused on particle trajectories beneath irrotational Stokes waves. Carter et al. [6] primarily use the Nonlinear Schrödinger equations to describe the surface of a Stokes wave and study the paths of the particles beneath this wave, obtaining similar results to those for a Stokes wave described by the Euler equations. Vanneste and Young [29] show that the Stokes drift can be decomposed into a solenoidal component, which simplifies the analysis of the Stokes drift and particle paths beneath Stokes waves. Other authors consider waves with constant vorticity, which can represent a realistic flow when waves are long compared to the depth or short compared to the length scale of the vorticity distribution [27]. Van den Bremer and Breivik [5] studied Stokes drift through experimental studies using photographic techniques in the laboratory to compare theoretical and experimental results. They also discussed three main areas of application for Stokes drift: in the coastal zone, in Eulerian models, and in models of tracer transport, such as oil and plastic pollution. Abrashkin and Pelinovsky [2] analyzed the Stokes drift beneath two types of waves, Stokes waves and Gerstner waves, and showed a relationship between Gerstner waves, Stokes waves, and Stokes drift. Specifically, the quadratic approximation of particle trajectories beneath a Stokes wave is a superposition of the vorticity flow of the Gerstner wave and the shear flow of the Stokes drift. Weber [30] demonstrated that the

Stokes drift beneath a Gerstner wave is zero using a nonlinear Lagrangian formulation.

All the studies described in the previous paragraph are focused on the behavior of particles beneath a water free surface wave. In some applications, it is useful to combine two areas of study: hydrodynamics and electrical engineering. This subject of study is known as electrohydrodynamics (EHD), and it focuses on fluid motion under the influence of an electric field. This area of study can be widely applied in chemical engineering contexts, such as cooling systems in conducting pumps [18], coating processes [20], and more. Flamarion and collaborators [13, 17] coupled normal electric fields and vorticity to study the effect of electric fields on the velocity field.

To the best of our knowledge, there are no studies in the literature on the effect of the electric field on the Stokes drift. To fill this gap, in this work, we are interested in numerically studying the Stokes drift of a particle beneath an irrotational Stokes wave considering the action of a normal electric field acting on the fluid. We consider a dielectric fluid in a two-dimensional space, bounded below by an electrode and above by a conducting passive gas, which in turn is bounded above by another electrode. A potential difference is applied between the electrodes such that the electric field is imposed in the direction perpendicular to the undisturbed fluid surface. This configuration is well known for destabilizing the interface between the fluids. Our aim is to numerically study the Stokes drift beneath irrotational waves under the influence of normal electric fields and investigate some properties of the kinetic energy on particle trajectories. More specifically, we used conformal mapping and pseudo-spectral numerical methods to compute the particle trajectories and evaluate the Stokes drift. Our results indicate that the Stokes drift remains unchanged with variation of the electric field.

The article is structured as follows: The mathematical formulation is presented in Section 2. The linear case and the properties of Stokes Drift are studied in Section 3. The nonlinear problem and the numerical methods are presented section 4. Results are presented in Sections 5 and 6. Finally, concluding remarks are provided in Section 7.

## 2 Mathematical Formulation

Consider an inviscid and incompressible dielectric fluid bounded by wall electrodes on top and bottom and surrounded by a conducting gas as we can see in Figure 1. In this case the fluid is conditioned to the action of an normal electric field ( $\vec{E} = \nabla V$ ).

Let  $\vec{U} = \nabla\phi$  represent the irrotational velocity field of the fluid motion. Denote the fluid surface by  $\eta(x, y, t)$ , where  $\lambda$  is the wavelength and  $c$  is the wave speed. By introducing the change of variables  $X(t) = x(t) - ct$  and  $Y(t) = y(t)$ , we can express the fluid surface as  $\eta(x, y, t) = \eta(X, Y)$ . Then, following the approach in [13], we can express the Euler governing equations in dimensionless form, using the electric field

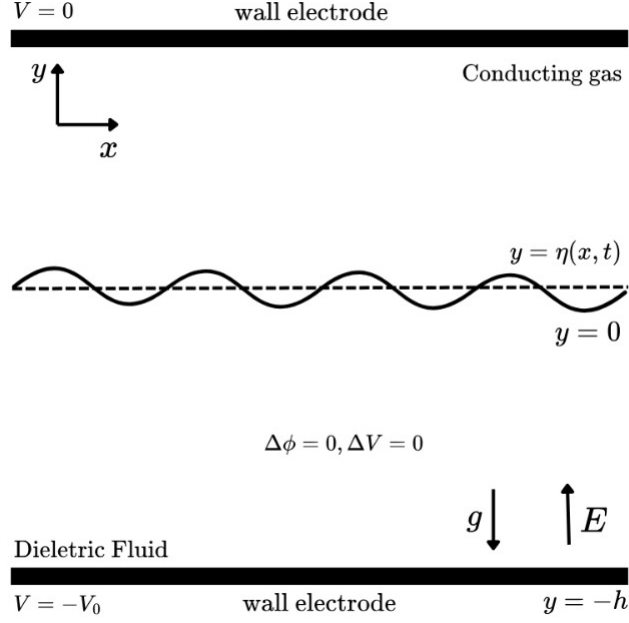


**Figure 1:** Physical context of the problem

and speed potentials as follows

$$\begin{aligned}
\Delta\phi &= 0 \quad \text{in} \quad -1 < Y < \eta(X) \\
\Delta V &= 0 \quad \text{in} \quad -1 < Y < \eta(X) \\
-c\eta_X + \phi_X\eta_X &= \phi_Y \quad \text{for} \quad Y = \eta(X) \\
\phi_Y &= 0 \quad \text{for} \quad Y = -1 \\
V &= 0 \quad \text{for} \quad Y = \eta(X) \\
V &= -1 \quad \text{for} \quad Y = -1.
\end{aligned} \tag{1}$$

In addition to governing equations, we have the dynamic bound condition:

$$-c\phi_X + \frac{1}{2}(\phi_X^2 + \phi_Y^2) + \eta - \sigma \frac{\eta_{XX}}{(1 + \eta_x^2)^{\frac{3}{2}}} + M_e = B, \tag{2}$$

where  $B$  is Bernoulli's constant and  $M_e$  represents the Maxwell stress tensor given by

$$M_e = \frac{E_b}{2(1 + \eta_x^2)} ((1 - \eta_x^2)(V_Y^2 - V_X^2) - 4\eta_x V_X V_Y) = \frac{E_b}{2} |\nabla V|^2. \tag{3}$$

The parameters  $\tau$  and  $E_b$  represent the nondimensional Bond and Electric Bond numbers, respectively, defined as follows

$$\sigma = \frac{T}{\rho g h^2}, \quad E_b = \frac{\epsilon_1 V_0^2}{\rho g h^3} \tag{4}$$

The hydrodynamic pressure in fluid body is computed through the Bernoulli equation

$$p = -(-c\phi_x + \frac{1}{2}(\phi_x^2 + \phi_y^2) + Y - B). \tag{5}$$

In the next section, we address the problem of waves with infinitesimally small amplitude (linear waves).

### 3 The linear problem

In this section, a linear theory is developed from the governing equations (1). A trivial solution is

$$\begin{cases} \eta_0(X) = 0, \\ \phi_0(X, Y) = 0, \\ V_0(X, Y) = Y, \end{cases}$$

which is perturbed by a small disturbance, namely

$$\begin{cases} \eta_0(X) = \varepsilon \hat{\eta}, \\ \phi_0(X, Y) = \varepsilon \hat{\phi}, \\ V_0(X, Y) = Y + \varepsilon \hat{V}. \end{cases}$$

Here,  $\varepsilon$  is a small parameter that measures the wave amplitude. Solving Laplace equations with boundary conditions as described in (1) yields

$$\begin{cases} \hat{\eta}(X) = \Re\{Ae^{ikX}\}, \\ \hat{\phi}(X, Y) = \Re\{Be^{ikX} \cosh(k(Y+1))\}, \\ \hat{V}(X, Y) = \Re\{De^{ikX} \sinh(k(Y+1))\}. \end{cases} \quad (6)$$

Here,  $A$ ,  $B$ , and  $D$  are unknown constants, and  $k = 2\pi/\lambda$  is the wavenumber. By linearizing the dynamic and kinematic boundary conditions, we obtain

$$\begin{cases} A = \varepsilon a, \\ B = \frac{-iAc}{\sinh(k)}, \\ D = \frac{-A}{\sinh(k)}, \end{cases}$$

and the linear dispersion relation

$$c = \pm \frac{\sqrt{4k \tanh(k)(1 + \sigma k^2) - 4k^2 E_b}}{2k}.$$

From this point on, we only consider the positive value of  $c$ , i.e., the right moving waves.

To study the effect of the electric field on particle trajectories, the velocity field  $\vec{U}$  is derived from (1) and (6)

$$\begin{cases} \hat{\phi}_X(X, Y) = \frac{kAc \cos(kX) \cosh(k(Y+1))}{\sinh(k)} \\ \hat{\phi}_Y(X, Y) = \frac{kAc \sin(kX) \sinh(k(Y+1))}{\sinh(k)}. \end{cases} \quad (7)$$

Therefore, the path of the particles that move with wave speed is given by the following dynamical system

$$\begin{cases} \frac{dX}{dt} = \phi_X(X, Y) - c, \\ \frac{dY}{dt} = \phi_Y(X, Y). \end{cases} \quad (8)$$

### 3.1 Stokes Drift

In this section, we will analytically define the Stokes drift and establish some of its properties and theorems. To begin, we recall the definition of Stokes drift.

**Definition 3.1.** Let  $(X(t), Y(t))$  be a solution of the ODE system (17) with initial condition  $(X_0, Y_0)$ ,  $Y_0 \in [-1, 0]$ . The time needed to this solution intercepts the line  $x = X_0 - \lambda$  is called **Drift Time** and is denoted by  $\tau(Y_0)$ .

This Drift time can also be seen as the time needed to the particle travel a wave phase.

**Remark 3.1.** Let  $\tau(Y_0)$  be a Drift time of a particle trajectory then:

- The Drift time depends only of the initial condition  $Y_0$ ;
- By symmetry we have that:

$$X(\tau(Y_0)) = X(0) - \lambda \quad \text{and} \quad Y(\tau(Y_0)) = Y_0.$$

In Constantin [7] we can see a formula to calculate the Drift time of a particle trajectory:

$$\tau(Y_0) = \int_{-\lambda/2}^{\lambda/2} \frac{dx}{c - \phi_X(X, Y_0)} \quad (9)$$

Then we can enunciate the following theorem

**Theorem 3.1.** The Drift time  $\tau(Y_0)$  of fluid particle path satisfies the inequality

$$\frac{\lambda}{c} < \tau(Y_0) \leq \int_{-\lambda/2}^{\lambda/2} \frac{1}{c - \phi_X(X, \eta(X))} dx$$

where  $\lambda/c$  is the wave period.

*Proof.* A proof of this theorem can be seen in [21]. □

With this concept we introduce the following definition.

**Definition 3.2.** Let  $(X(t), Y(t))$  be a solution of the ODE system (17) with initial condition  $(X_0, Y_0)$ ,  $Y_0 \in [-1, 0]$  and Drift time  $\tau(Y_0)$ . We define as **Stokes Drift** of this solution the distance between  $(x(0), y(0))$  and  $(x(\tau(Y_0)), y(\tau(Y_0)))$  where  $x(t) = X(t) + ct$  and  $y(t) = Y(t)$ .

We can also calculate the Stokes Drift of a particle using the proposition.

**Proposition 3.1.** Let  $(X(t), Y(t))$  be a solution of the ODE system (17) with initial condition  $(X_0, Y_0)$ ,  $Y_0 \in [-1, 0]$  and Drift time  $\tau(Y_0)$ . For a fixed  $Y_0$  we have that:

$$\text{Drift} = ct - \lambda > 0.$$

*Proof.* As  $Y_0$  is fixed, for simplicity we will denote the Drift time  $\tau(Y_0)$  as only  $\tau$ . By definition we know that:

$$Drift = \sqrt{(x(\tau) - x(0))^2 - (y(\tau) - y(0))^2}$$

By Remark 3.1 and passing to the moving frame  $x = X + ct$ ,  $y = Y$ :

$$\begin{aligned} Drift &= \sqrt{(X(\tau) + c\tau - X(0))^2 - (Y(\tau) - Y(0))^2} \\ &= \sqrt{(X(0) - \lambda + c\tau - X(0))^2} \\ &= c\tau - \lambda. \end{aligned}$$

And we know from Theorem 3.1:

$$\frac{\lambda}{c} < \tau \Rightarrow c\tau > \lambda \Rightarrow c\tau - \lambda > 0.$$

□

**Remark 3.2.** *The Proposition 3.1 ensures that particle paths are not closed beneath Stokes waves. Moreover, there is a closed particle path if and only if  $\tau = \lambda/c$ .*

As well we can investigate some geometric parameters of a particle trajectory that are defined by:

**Definition 3.3.** *Let  $(X(t), Y(t))$  be a solution of the system (8) with initial conditions  $(X_0, Y_0)$ ,  $Y_0 \in [-1, 0]$  and Drift time  $\theta(Y_0)$ . We'll define three parameters:*

1.  $d_1$  is the Stokes Drift of the trajectory;
2.  $d_2$  is the distance between  $(x(t_1), y(t_1))$  and  $(x(t_2), y(t_2))$  such that  $t_1, t_2 \in [0, \theta]$ ,  $x(t_1) = \min_{t \in [0, \theta]} x(t)$  and  $x(t_2) = \max_{t \in [0, \theta]} x(t)$ . Can be seen as the maximum horizontal distance;
3.  $d_3$  is the distance between  $(x(t_3), y(t_3))$  and  $(x(t_4), y(t_4))$  such that  $t_3, t_4 \in [0, \theta]$ ,  $y(t_3) = \min_{t \in [0, \theta]} y(t)$  and  $y(t_4) = \max_{t \in [0, \theta]} y(t)$ . Can be seen as the maximum vertical distance.

## 4 The nonlinear problem

For the nonlinear case of solving system (1), we use a conformal mapping formulation. This involves finding a map that transforms our physical domain into a rectangular one, which is more suitable for numerical simulations. The procedure has appeared in different works in the literature [11, 12, 16], here we only summarise the main steps.

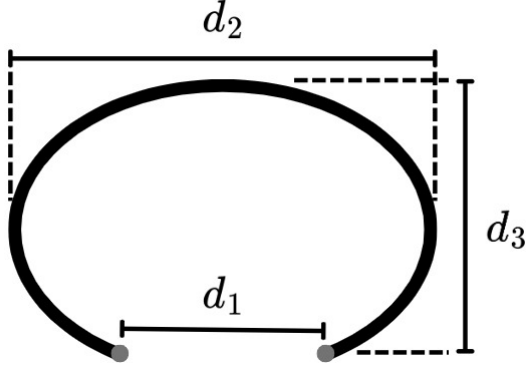


**Figure 2:** Geometric parameters indicating the aspect ratio of an trajectory

Consider the physical domain as  $\Gamma = \{(X, Y) \in \mathbb{C}; -\frac{\lambda}{2} < X < \frac{\lambda}{2}, -1 < Y < \eta(X)\}$  and the canonical domain  $\tilde{\Gamma} = \{(\xi, \zeta) \in \mathbb{C}; -\frac{L}{2} < \xi < \frac{L}{2}, -D < \zeta < 0\}$ . Then we need to find a map  $Z : \tilde{\Gamma} \rightarrow \Gamma$  such that  $Z(\xi, \zeta) = \tilde{X}(\xi, \zeta) + i\tilde{Y}(\xi, \zeta)$  and  $Z$  is conformal.

From some algebraic manipulations in (1), using Fourier transforms and the hypothesis of  $Z$  being conformal yields

$$\begin{cases} \tilde{X}(\xi, \zeta) = -\mathcal{F}_{k \neq 0}^{-1} \left[ \frac{i \cosh(k(D+\zeta))}{\sinh(kD)} \hat{\mathbf{Y}}(k) \right] + \xi \\ \tilde{Y}(\xi, \zeta) = \mathcal{F}_{k \neq 0}^{-1} \left[ \frac{i \sinh(k(D+\zeta))}{\sinh(kD)} \hat{\mathbf{Y}}(k) \right] + \tilde{\mathbf{Y}}(0) + \zeta. \end{cases} \quad (10)$$

where  $\tilde{\mathbf{Y}}(\xi) = \tilde{Y}(\xi, \zeta = 0)$  and  $\mathcal{F}[\cdot]$  is defined on the space of integrable functions in  $[-L/2, L/2]$  with the following notations:

- $\mathcal{F}[f(\xi)] = \hat{f}(k_j) = \frac{1}{L} \int_{-\frac{L}{2}}^{\frac{L}{2}} f(\xi) e^{-ik_j \xi} d\xi;$
- $\mathcal{F}^{-1}[\hat{f}(k)] = f(\xi) = \sum_{j \in \mathbb{Z}} \hat{f}(k_j) e^{ik_j \xi};$
- $k_j = \frac{2\pi}{L} j, j \in \mathbb{Z}.$

In this work, we assume that  $L = \lambda$  (wavelength) and that gives:

$$D = \langle \tilde{\mathbf{Y}} \rangle + 1, \quad (11)$$

that is extremely important to the manipulations needed for the numerical scheme.

To find the free surface elevation we make use of the Hilbert operator  $\mathcal{C}[\cdot]$  defined as

$$\mathcal{C}[f(\xi)] = \mathcal{C}_0[f(\xi)] + \lim_{k \rightarrow 0} i \coth(kD) \hat{f}(k),$$

where,

$$\mathcal{C}_0 = \mathcal{F}^{-1}[\mathcal{H}\mathcal{F}[\cdot]]$$

and,

$$\mathcal{H}(k) \stackrel{\text{def}}{=} \begin{cases} i \coth(kD), & k \neq 0, \\ 0, & k = 0. \end{cases}$$



With the use of this operator, we can get an important relation between  $\tilde{\mathbf{Y}}(\xi)$  and  $\tilde{\mathbf{X}}(\xi) = X(\xi, 0)$ , that is:

$$\tilde{\mathbf{X}}_\xi = 1 - \mathcal{C}_0[\tilde{\mathbf{Y}}_\xi]$$

Now we proceed to translate from the boundary conditions at the free surface to ones in the canonical domain.

As mentioned previously the velocity field is irrotational, i.e,  $\vec{U} = \nabla\phi$  and  $\tilde{\phi}(\xi, \zeta) = \phi(\tilde{X}(\xi, \zeta), \tilde{Y}(\xi, \zeta))$ . As well we denote as  $\psi(\xi, \zeta) = \psi(X, Y)$  an harmonic conjugate of  $\phi(X, Y)$ .

$$\begin{cases} \phi_X(X, Y) = \frac{1}{|J|}(\tilde{\Phi}_\xi \tilde{\mathbf{X}}_\xi + \tilde{\Psi}_\xi \tilde{\mathbf{Y}}_\xi), \\ \phi_Y(X, Y) = \frac{1}{|J|}(\tilde{\Phi}_\xi \tilde{\mathbf{Y}}_\xi - \tilde{\Psi}_\xi \tilde{\mathbf{X}}_\xi), \end{cases} \quad (12)$$

Following the approach used in [13, 16], the free surface is determined by solving the system of equations

$$\begin{aligned} G(\tilde{\mathbf{Y}}(\xi), c, D, B) &= 0, \\ \frac{-c^2}{2} + \frac{c^2}{2J} + \tilde{\mathbf{Y}} + \sigma \frac{\tilde{\mathbf{X}}_\xi \tilde{\mathbf{Y}}_{\xi\xi} - \tilde{\mathbf{Y}}_\xi \tilde{\mathbf{X}}_{\xi\xi}}{J^{3/2}} + \frac{E_b}{2D^2J} - B &= 0, \end{aligned} \quad (13)$$

where  $J = X_\xi^2 + Y_\xi^2$  is the Jacobian of the map. Hence, as unknowns, we have  $\mathbf{Y}(\xi)$ ,  $c$ ,  $B$  and  $D$ , and therefore (13) must be supplemented by three conditions: we fix the wave height  $H$  through

$$\tilde{\mathbf{Y}}(0) - \tilde{\mathbf{Y}}(\lambda/2) = H, \quad (14)$$

and we impose a mean-zero wave profile in the physical space,

$$\int_{-\lambda/2}^0 \tilde{\mathbf{Y}} \tilde{\mathbf{X}}_\xi d\xi = 0, \quad (15)$$

as well the depth condition

$$D = \langle \tilde{\mathbf{Y}} \rangle + 1, \quad (16)$$

As we seek to study the effect of the electric field in the trajectory of fluid particles beneath this wave then we need to solve

$$\begin{cases} \frac{dX}{dt} = \phi_X(X, Y) - c \\ \frac{dY}{dt} = \phi_Y(X, Y). \end{cases} \quad (17)$$

In the canonical domain, the corresponding trajectory  $(\xi(t), \zeta(t))$ , such that

$$(X(t), Y(t)) = (\tilde{X}(\xi(t), \zeta(t)), \tilde{Y}(\xi(t), \zeta(t))), \quad (18)$$

is obtained from

$$\begin{cases} \frac{d\xi}{dt} = \tilde{\phi}_\xi - c\tilde{Y}_\zeta \\ \frac{d\zeta}{dt} = \tilde{\phi}_\zeta - c\tilde{Y}_\xi. \end{cases} \quad (19)$$

## 4.1 Numerical Methods

In this section, we present the method and follow it with the results of numerical experiments across a range of amplitude, wavelength, and electric bound parameters. In the remainder of the paper, the depth ( $D$ ) is fixed at 1 and the wavelength ( $\lambda$ ) is fixed at  $2\pi$ . We will focus on this intermediate-depth case and vary the steepness parameter  $\varepsilon = H/\lambda$ .

Recall that once the  $\lambda$ -periodic wave elevation  $\mathbf{Y}$  is determined, we can directly solve the full solution in the canonical domain. To achieve this, we seek to numerically solve the equations (13)-(16). Define an equally spaced partition of  $\xi$  at  $\zeta = 0$  in the canonical domain

$$\xi_j = -\frac{\lambda}{2} + (j-1)\Delta\xi, \quad j = 1, \dots, N, \quad \text{where } \Delta\xi = \lambda/N.$$

The number of grid points is  $N = 2^p$  with  $p \in \mathbb{Z}$ . Let  $\tilde{\mathbf{Y}}_j := \tilde{\mathbf{Y}}(\xi_j)$  and  $\tilde{\mathbf{X}}_j := \tilde{\mathbf{X}}(\xi_j)$ , and impose even symmetry about  $\xi = 0$  by taking  $\tilde{\mathbf{Y}}_j = \tilde{\mathbf{Y}}_{N-j+2}$  for  $j = N/2 + 2, \dots, N$ . In this way, by discretizing (13), we obtain a set of  $N/2 + 1$  equations for  $N/2 + 4$  unknowns. The missing equations are provided by the discrete form of equations (14)-(16). The discretized system is then given by

$$\begin{cases} G_j(\tilde{\mathbf{Y}}_j, c, D, B) = 0, \\ G_{N/2+2}(\tilde{\mathbf{Y}}_j, c, D, B) = \tilde{\mathbf{Y}}_{N/2+1} - \tilde{\mathbf{Y}}_1 - H = 0, \\ G_{N/2+3}(\tilde{\mathbf{Y}}_j, c, D, B) = \frac{\tilde{\mathbf{Y}}_1 \tilde{\mathbf{X}}_{\xi_1} + \tilde{\mathbf{Y}}_{N/2+1} \tilde{\mathbf{X}}_{\xi_{(N/2+1)\Delta\xi}}}{2} + \Delta\xi \sum_{j=2}^{N/2} \tilde{\mathbf{Y}}_j \tilde{\mathbf{X}}_{\xi_j} = 0, \\ G_{N/2+4}(\tilde{\mathbf{Y}}_j, c, D, B) = \frac{2}{N} \left( \frac{\tilde{\mathbf{Y}}_1 + \tilde{\mathbf{Y}}_{N/2+1}}{2} + \sum_{j=2}^{N/2} \tilde{\mathbf{Y}}_j \right) + 1 - D = 0. \end{cases} \quad (20)$$

It should be noted that this discretization replaces all derivatives and non-local linear operators with their discretized Fourier symbols. As a result, their action is computed with spectral accuracy in Fourier space, while all nonlinearities are computed in real space at the partition points.

The system (20) is solved by Newton's method, with linear waves as initial guess

$$\mathbf{Y}(X) = 10^{-5} \cos(kX), \quad c = \frac{\sqrt{4k \tanh(k)(1 + \sigma k^2) - 4k^2 E_b}}{2k}, \quad D = 1, \quad B = 0,$$

and different values of  $\tau$ ,  $E_b$ , and  $\varepsilon$  are used for our numerical simulations. The stopping criterion for Newton's Method is given by

$$\frac{\sum_{j=1}^{N/2+4} |G_j|}{N/2+4} < 10^{-10}.$$

Particle trajectories are determined by integrating the ODE system (19) in the canonical domain using the fourth-order Runge-Kutta method. These trajectories are then mapped onto the moving frame  $(X(t), Y(t))$ . To study the paths in the laboratory frame of reference, we use the change of variables  $x(t) = X(t) + ct$  and  $y(t) = Y(t)$ .

## 5 Numerical results

In this section, we explore some numerical experiments regarding the variation of the electric field in wave generation to discuss the geometric parameters of the particle path, drift time, and wave speed. Consider  $\varepsilon = 0.09$ ,  $\sigma = 0$ , and the initial condition  $(-\pi, -D/2)$  to find the particle trajectory. Note that  $c$  depends on  $E_b$  and  $\sigma$ . Given  $\tau = 0$  and  $k = 2\pi/\lambda = 1$ , and imposing  $c \in \mathbb{R}$ , we obtain an upper limit for  $E_b$  as follows

$$E_b \leq \tanh(1) \approx 0.761594155955765$$

Our simulations show that varying the  $E_b$  parameter decreases the wave speed and increases the drift time, as illustrated in Figure 3. Additionally, simulating the tra-

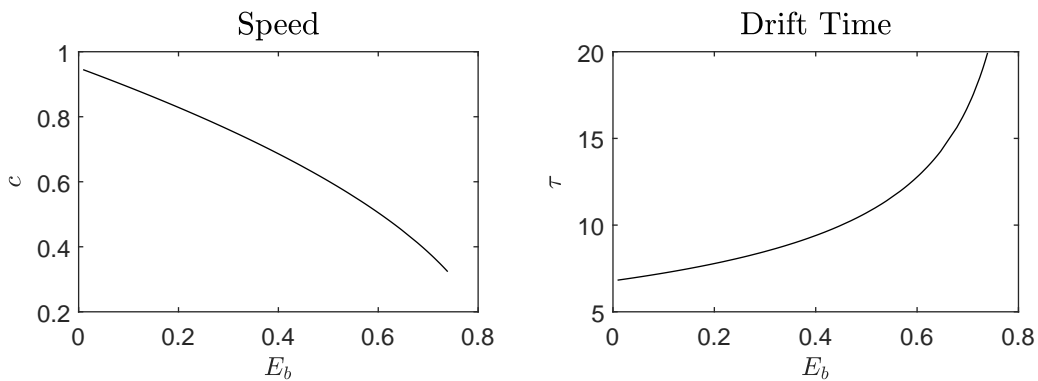


**Figure 3:** Speed and drift time with variation of  $E_b$

jectory of particles starting from the same initial location with varying  $E_b$  in wave generation results in identical paths and Stokes drift for all  $E_b$  values. This indicates that increasing the effect of the electric field does not alter the particles' paths beneath the wave. This is further demonstrated in Figure 4.

To investigate the geometric parameters of the particle trajectory, we use the wave generated by  $E_b^* = 0$  as a reference and obtain the following parameters

$$\begin{aligned} d_1^* &= 0.165243806395989, \\ d_2^* &= 0.495211466893694, \\ d_3^* &= 0.190316620280615, \\ \tau^* &= 6.787715410459687, \\ c^* &= 0.950014654951160. \end{aligned}$$

So we can compute the relative error as

$$E_r(d_i) = \frac{|d_i - d_i^*|}{|d_i^*|}, \quad i = 1, 2, 3.$$

As shown in Figure 5, the relative error in the geometric parameters  $d_1$ ,  $d_2$ , and  $d_3$  is small. This indicates that the trajectory remains the same as  $E_b$  increases, although the particle slows down.

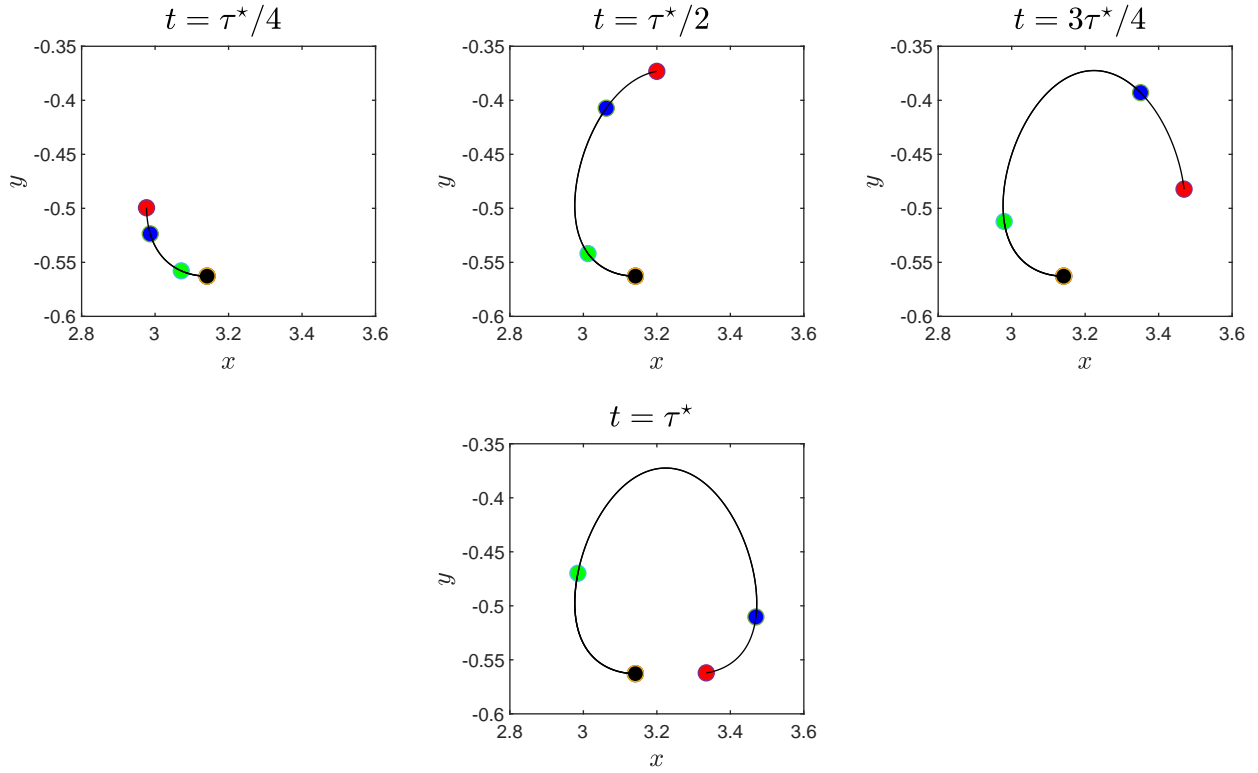


**Figure 4:** Snapshots of particle trajectory in time  $t$ . Red ( $E_b = 0$ ), Blue ( $E_b = 0.3$ ), Green ( $E_b = 0.7615$ ).

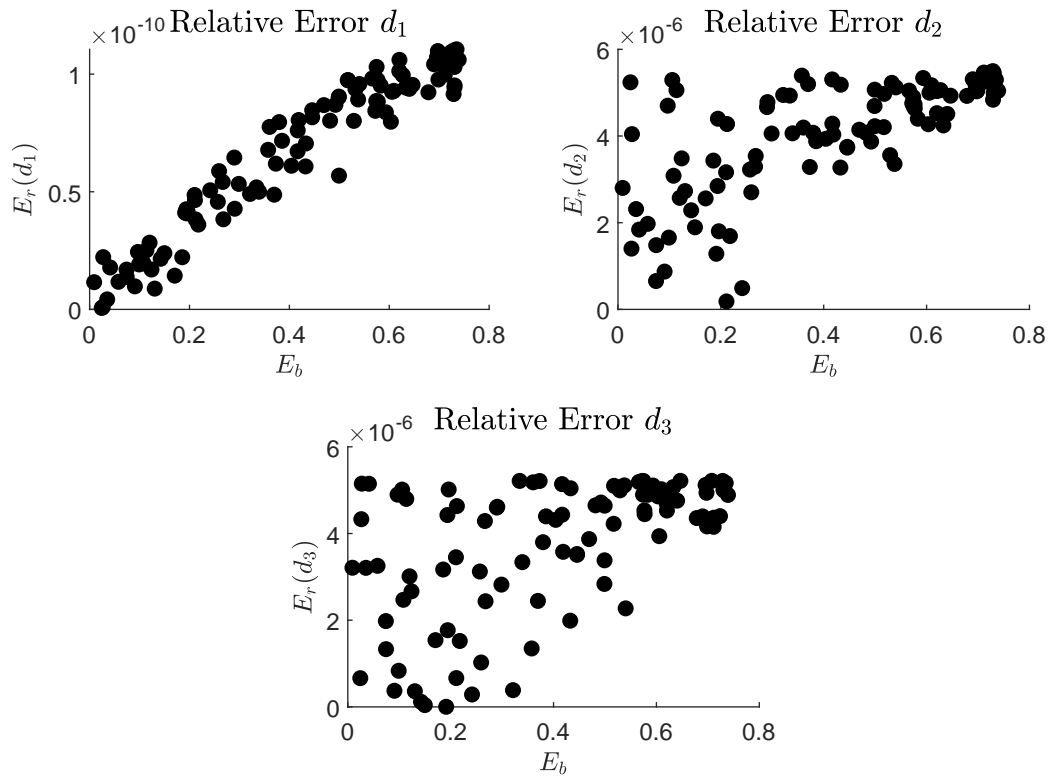


**Figure 5:** Relative errors

## 6 On the kinetic energy

In this section, we discuss the properties of the kinetic energy of particle trajectories previously analyzed. It is well known that kinetic energy is associated with the speed of moving bodies. Following the definition in [21], the total kinetic energy of a fluid particle initially located at  $(X_0, Y_0)$  over a drift time period is given by

$$\mathcal{E}(X_0, Y_0) = \int_0^{\tau(Y_0)} \left[ \left( \frac{dX}{dt} + c \right)^2 + \frac{dY^2}{dt} \right] dt$$

Here, we use the moving frame  $X = x - ct$ ,  $Y = y$  as a reference. Thus, the total kinetic energy in the moving frame over a drift time period is:

$$E(X_0, Y_0) = \int_0^{\tau(Y_0)} \left[ \frac{dX^2}{dt} + \frac{dY^2}{dt} \right] dt$$

Based on [21], we state the following theorem:

**Theorem 6.1.** *Let  $X(t)$  and  $Y(t)$  be solutions of the system (17) with initial conditions  $(X_0, Y_0)$  and  $\tau(Y_0)$  be the drift time of this trajectory. Then the function  $\mathcal{E}(X_0, Y_0)$  is convex and non-decreasing, depending solely on  $Y_0$  and independent of the initial location  $X_0$ . The function  $E(X_0, Y_0)$  is constant and equal to  $c\lambda/2$ .*

*Proof.* A proof of this theorem can be found in [21]. □

We investigate this theorem numerically using 100 simulations of particles initially located at  $X_0 = \pi$  with  $Y_0$  varying through the interval  $[0, -1]$ . The results are as follows:

1. For one wave without the effect of the electric field ( $E_b = 0$ ), our numerical experiments agree with Theorem 6.1, as shown in Figure 6.
2. For three waves with different electric fields ( $E_b = 0, 0.3, 0.7$ ), Figure 7 shows that varying  $E_b$  maintains the properties of kinetic energy as stated in Theorem 6.1, with increasing  $E_b$  resulting in decreased kinetic energy in both frames.
3. For three waves with different heights ( $\varepsilon_1 = 0.001$ ,  $\varepsilon_2 = 0.04$ ,  $\varepsilon_3 = 0.09$ ) without the effect of the electric field, Figure 8 shows that varying the steepness  $\varepsilon$  also preserves the kinetic energy properties, with decreasing  $\varepsilon$  leading to lower kinetic energy. For the wave with steepness  $\varepsilon = 0.001$ , the kinetic energy  $\mathcal{E}$  is small compared to the others, so we include a zoomed-in figure.

Note that these simulations depend on the drift time  $\tau(Y_0)$  of particle trajectories at different initial locations  $(X_0, Y_0)$ . Our experiments show that the variation of  $Y_0$  in the drift time is non-decreasing, as shown in Figure 9. This simulation was conducted with  $\varepsilon = 0.09$ ,  $E_b = 0$ , and  $\sigma = 0$ .

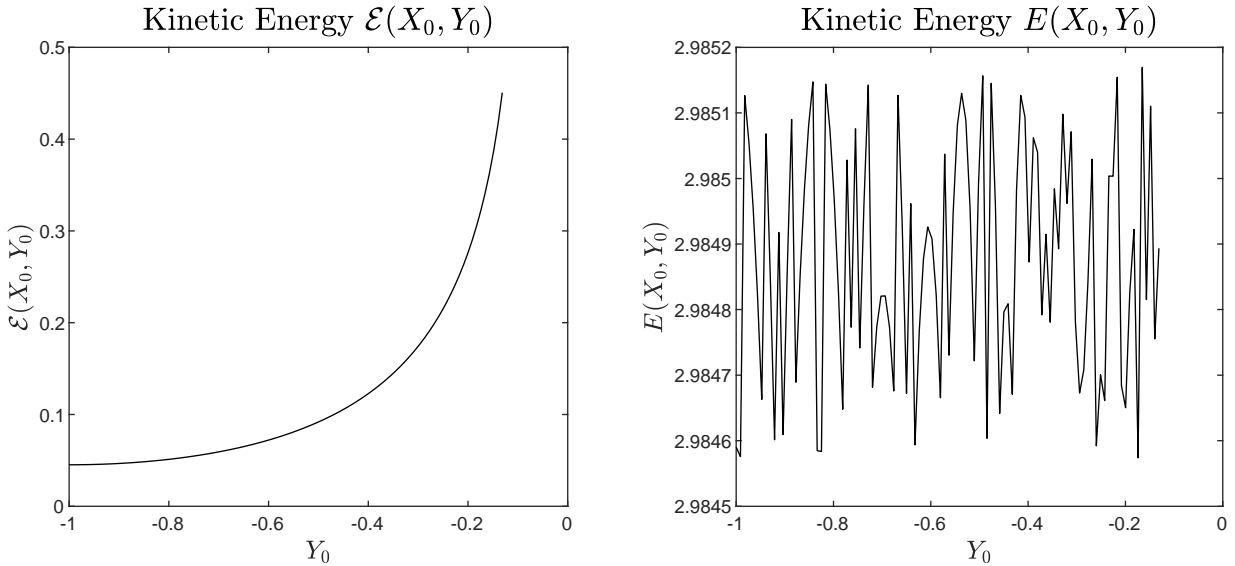


Figure 6: Kinetic Energy (1st case)

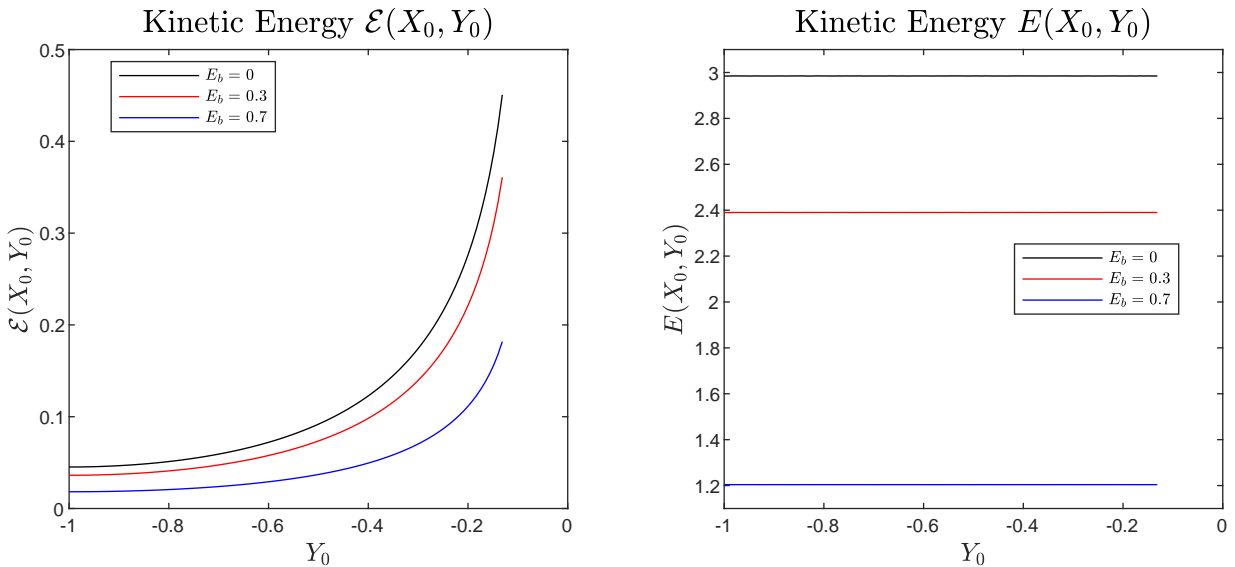
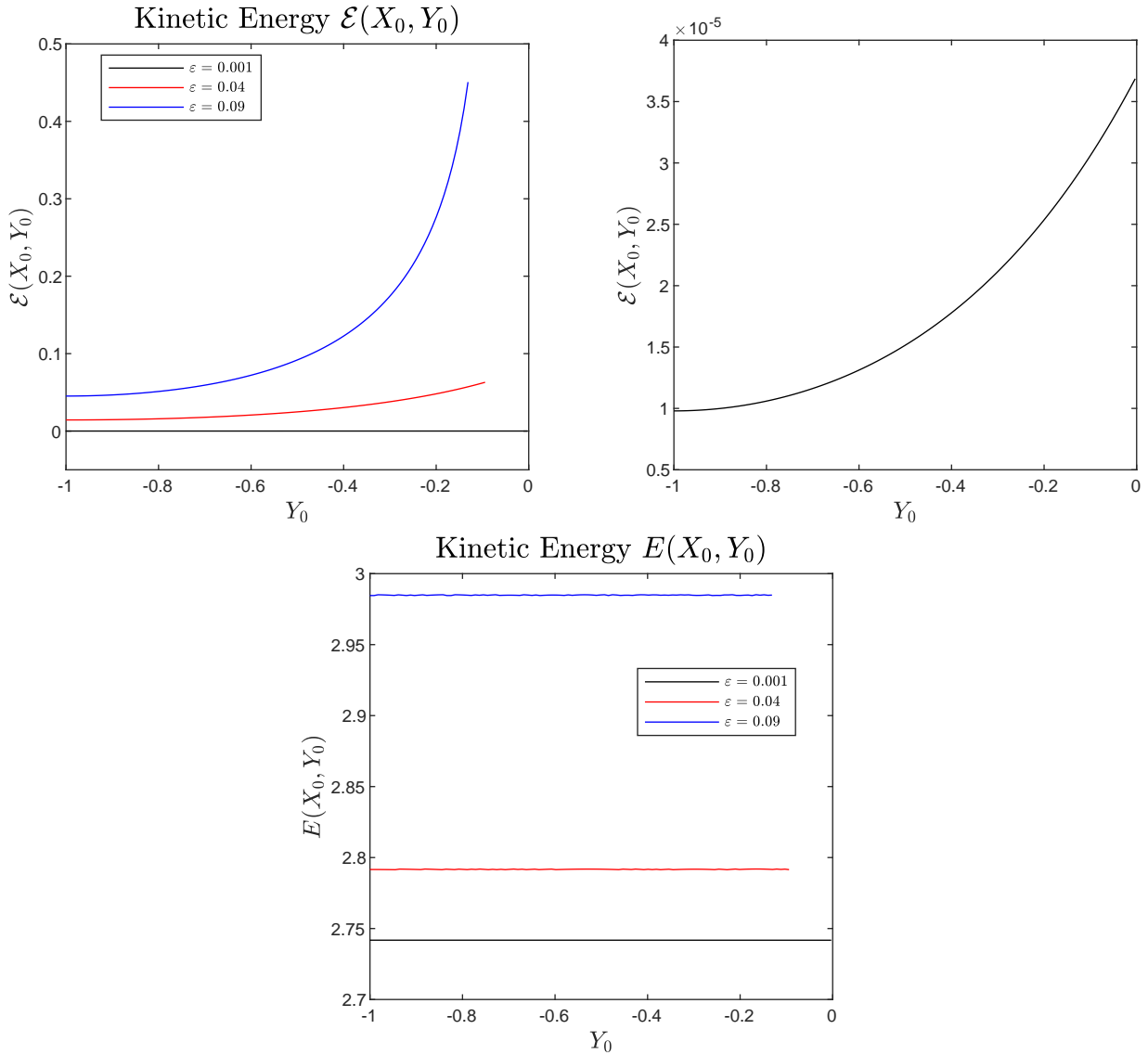


Figure 7: Kinetic Energy (2nd case)

## 7 Conclusion

In this work, we study the effects of varying the Electric Bound Number ( $E_b$ ) on the Stokes Drift of a particle beneath a Stokes Wave, as modeled by Euler's equations, and examine some properties of the kinetic energy in particle trajectories beneath the wave at different initial locations.

First, we define the governing equations for the fluid surface in terms of potential functions for the velocity and electric fields. By linearizing these equations, we obtain useful results for generating waves in the nonlinear case. Next, we define the drift time, Stokes Drift, and establish some properties of these two fundamental concepts for this work. For the numerical scheme, we employed a conformal mapping technique to solve the nonlinear governing equations in a simpler domain, facilitating the extraction of



**Figure 8:** Kinetic Energy (3rd case)

results.

Our numerical results indicate that the electric field acting on the wave slows down the particle trajectory while maintaining the same shape. Additionally, the kinetic energy is a non-decreasing convex function in the moving frame and remains constant in the laboratory frame.

## Acknowledgements

The author L.P.P. is grateful for the financial support provided by CAPES Foundation (Coordination for the Improvement of Higher Education Personnel) during part of the development of this work. The work of M.V.F. and R.R.Jr was supported in part by National Council Scientific and Technological Development (CNPq) under Chamada CNPq/MCTI/No 10/2023-Universal.

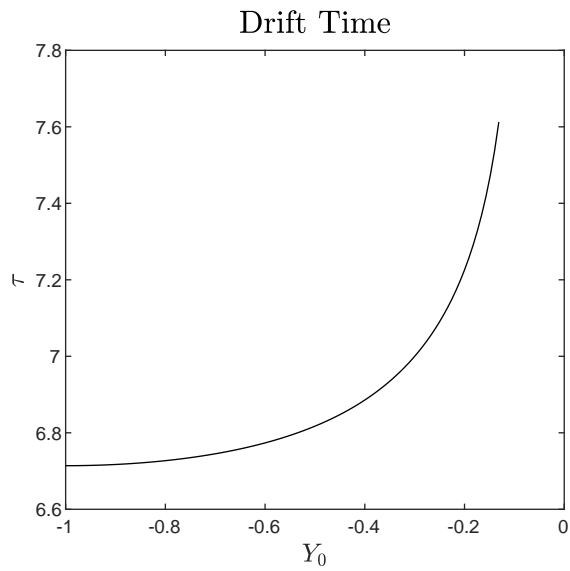


**Figure 9:** Drift Time with  $Y_0$  variation

## Declarations

## Conflict of interest

The authors state that there is no conflict of interest.

## Data availability

Data sharing is not applicable to this article as all parameters used in the numerical experiments are informed in this paper.



# References

- [1] ALFATIH A., KALISCH, H., Reconstruction of the pressure in long-wave models with constant vorticity. *Eur. J. Mech. B Fluids* **37** (2013) 187-194.
- [2] ABRASHKIN, A. A, PELINOVSKY, E. N., On the relation between Stokes drift and the Gerstner wave. *Physics-Uspekhi* **61** (2018) 307-312.
- [3] AIRY, G. B., Tides and Wave. *Encyclopaedia Metropolitana* **5** (1842).
- [4] BORLUK, H., KALISCH, H., Particle dynamics in the KdV approximation. *Wave Motion* **49**, (2012) 691-709.
- [5] VAN DEN BREMER, T. S., BREIVIK, Ø., Stokes Drift. *Phil. Trans. of the R.S A: Math., Phys. and Eng. Sciences* **376** (2017) 20170104.
- [6] CARTER, J. D., CURTIS, C. W, KALISCH H., Particle Trajectories in Nonlinear Schrödinger Models. *Water Waves* **2** (2019) 31-57.
- [7] CONSTANTIN, A., The trajectories of particles in Stokes waves. *Invent. Math.* **166** (2006) 523-535.
- [8] CONSTANTIN, A., VILLARI, G., Particle trajectories in linear water waves. *J. Math. Fluid Mech.* **10** (2008) 1336-1344.
- [9] CONSTANTIN, A., STRAUSS, W., Pressure beneath a Stokes wave. *Comm. Pure Appl. Math.* **63** (2008) 533-557.
- [10] CRAIK, A., The origins of water wave theory. *Annu. Rev. Fluid Mech.* **36** (2004) 1-28.
- [11] DYACHENKO, A.I., KUZNETSOV, E.A., SPECTOR, M., ZAKHAROV, V.E., Analytical description of the free surface dynamics of an ideal fluid (canonical formalism and conformal mapping). *Phys. Lett. A* **221** (1996) 73-79.
- [12] FLAMARION, M. V., RIBEIRO-JR, R., An iterative method to compute conformal mappings and their inverses in the context of water waves over topographies. *Int. J. for Num. Methods in Fluids* **93** (2021) 3304-3311.
- [13] FLAMARION, M. V., GAO, T., RIBEIRO-JR, R., DOAK, A., Flow structure beneath periodic waves with constant vorticity under normal electric fields. *Physics of Fluids* **34** (2022) 127119.
- [14] FLAMARION, M. V., Complex flow structures beneath rotational depression solitary waves in gravity-capillary flows. *Wave Motion* **117** (2023) 103108.
- [15] FLAMARION, M. V., Stagnation points beneath rotational solitary waves in gravity-capillary flows. *Trends in Comp. and Applied Math.* **24** (2023) 265-274.

- [16] FLAMARION, M. V., KOCHURIN, E., RIBEIRO-JR, R., Fully nonlinear evolution of free-surface waves with constant vorticity under horizontal electric fields. *Mathematics* **11** (2023) 4467.
- [17] FLAMARION, M. V., GAO, T., RIBEIRO-JR, R., An investigation of the flow structure beneath solitary waves with constant vorticity on a conducting fluid under normal electric fields. *Physics of Fluids* **35** (2023) 037122.
- [18] GHOSHAL, U., MINER A. C., Cooling of high power density devices by electrically conducting fluids. *U.S. Patent* (2003) 6,658,861.
- [19] GREEN, G., On the motion of waves in a variable canal of small depth and width. *Trans. of the Cambridge Phil. Soc.* **6** (1838) 457-462.
- [20] GRIFFING, E. M., BANKOFF, S. G., MIKSIS, M. J., SCHLUTER R. A., Electrohydrodynamics of thin flowing films. *J. Fluids Eng.* **128** (2006) 276-283.
- [21] LI, J., YANG, S., Kinetic energy properties of irrotational deep-water Stokes waves. *arXiv:2406.00711v1*.
- [22] KHORSAND, Z., Particle trajectories in the Serre equations. *Appl. Math. Comput.*, **230** (2014) 35-42.
- [23] LONGUET-HIGGINS, M. S., The trajectories of particles in steep, symmetric gravity. *J. Fluid Mech.* **94** (1979) 497-517.
- [24] LONGUET-HIGGINS, M. S., Eulerian and Lagrangian aspects of surface waves. *J. Fluid Mech.*, **173** (1986) 683-707.
- [25] NACHBIN, A., RIBEIRO JR, R., A boundary integral formulation for particle trajectories in stokes wave. *Disc. and Cont. Dynamical Systems* **34** (2014) 3135-3153.
- [26] STOKES, G. G., On the theory of oscillatory waves. *Trans. Cambridge Phil. Soc.* **8** (1880) 411-455.
- [27] TELES DA SILVA, A. F., PEREGRINE, D. H., Steep, steady surface waves on water of finite depth with constant vorticity. *J. Fluid Mech* **195** (1988) 281-302.
- [28] URSELL, F., Mass transport in gravity waves. *Proc. Cambridge Phil. Soc.* **49** (1953) 145-150.
- [29] VANNESTE, J., YOUNG, W. R., Stokes drift and its discontents. *Phil. Trans. R. Soc. A* **380** (2022) 20210032.
- [30] WEBER, J. E. H., A Lagrangian study of internal Gerstner- and Stokes-type gravity waves. *Wave Motion* **88** (2019) 257-264.